Available online at www.sciencedirect.com
SCIENCE DIRECT
Icarus 182 (2006) 68–79
ICARUS
www.elsevier.com/locate/icarus

Infrared micro-spectroscopy of the martian meteorite Zagami: Extraction of individual mineral phase spectra

Ernesto Palomba [a,*], Alessandra Rotundi [b], Luigi Colangeli [c]

[a] *INAF, Istituto di Fisica dello Spazio Interplanetario, via del Fosso del Cavaliere 100, I-00133 Roma, Italy*
[b] *Università Parthenope, Via A. De Gasperi 5, I-80133 Napoli, Italy*
[c] *INAF, Osservatorio Astronomico di Capodimonte, Via Moiariello 16, I-80131 Napoli, Italy*

Received 19 January 2005; revised 19 December 2005

Available online 26 January 2006

Abstract

Zagami, a well characterized SNC meteorite, represents a reference sample to verify the feasibility of the non-destructive infrared micro-spectroscopy technique to extract spectral signatures from individual mineral phases in a meteorite sample. For the first time individual infrared spectra of the major mineral phases, in the 6000–600 cm^{-1} (1.67–16.7 μm) spectral interval, whose identification is confirmed by energy dispersive X-ray analysis and backscattered imaging, are measured. The signatures of the main mineral phases we identified in the Zagami chip are: (1) maskelynite characterized by broad and smooth Si–O vibrational bands in the 1000 cm^{-1} spectral region; (2) crystalline pyroxenes showing well defined fine structures; and (3) an oxide mineral phase with an almost featureless and flat spectrum. In the part of the spectrum centered around 2 μm, by analyzing the different positions of the Fe^{2+} bands, we were able to discern the high-Ca from the low-Ca pyroxene phases. This result demonstrates that by means of the infrared micro-spectroscopy technique it is possible to retrieve directly the composition of pyroxenes in the En–Fs–Wo system, without relying on the use of deconvolution techniques. In addition IR signatures due to water and aliphatic hydrocarbons were observed to be more abundant in the pyroxenes than in maskelynite. This could be an indication that the organic and water signatures are due to indigenous compounds in Zagami rather than laboratory contamination, however, further investigations are necessary before this conclusion can be confirmed.

Keywords: Mars; Meteorites; Spectroscopy; Mineralogy; Experimental techniques

1. Introduction

Conventional infrared spectroscopy is not suitable to extract spectral information of the individual mineral phases in bulk samples. In the past, with the intent to characterize individual mineral spectral features in some martian meteorites, attempts were made in laboratory to go towards the micro-scale, by reducing the spectrometer beam spot down to 1 mm (Bishop et al., 1998a, 1998b; Schade and Wasch, 1999). These analyses showed that it is possible to derive the dominant mineralogy of the samples, even if the spectra contain features that cannot be explained by an individual phase (Bishop et al., 1998a). One of the main intents of this work is to extract the individual IR spectral signatures of the main minerals composing a well studied sample such as the martian meteorite Zagami. Since the typical grain size in the shergottite–nakhlite–chassignite (SNC) suite samples, to which Zagami belongs, do not exceed few hundred of microns, the smallest beam available in common spectrometers (i.e., 1 mm) will inevitably spot different mineral phases and a deconvolution algorithm, such as the Modified Gaussian Model (MGM) (Sunshine et al., 1990), is necessary to extract the single phases (Sunshine et al., 1993; Schade and Wasch, 1999). To overcome this problem, we used an innovative approach for the extraction and the study of individual spectral signature of each mineral phase composing the heterogeneous sample, applying the infrared micro-spectroscopy (6000–600 $cm^{-1} \div 1.67$–16.7 μm) to a chip of Zagami. This technique has not been fully explored as a tool for analysis of extraterrestrial materials, only recently few at-

* Corresponding author. Fax: +39 081456710.
E-mail address: palomba@ifsi.rm.cnr.it (E. Palomba).

0019-1035/$ – see front matter
doi:10.1016/j.icarus.2005.12.009

tempts were made in order to characterize its potential and limitations (see, e.g., Suzuki et al., 2005; Morlok et al., 2004; Klima and Pieters, 2005). In this framework, our measurements add substantial material and could represent a robust reference for future micro-spectroscopy in situ analysis on Mars (e.g., Capaccioni et al., 2001; Lamartinie et al., 2003) or other planetary environments.

With this analytical technique we were able to show, for the first time, spectroscopic signatures of individual mineral phases present in Zagami. We obtained the spectral signatures of major pyroxene phases to which we applied the composition determination curves from Cloutis and Gaffey (1991) to infer their Ca content. In addition, to support and confirm the spectroscopic studies, we performed chemical analyses on the sampled region of the meteorite with an Energy Dispersive X-ray analyzer (EDX) attached to a Field Emission Scanning Electron Microscope (FESEM).

2. SNC's: Laboratory studies and connection with remote observations

The SNC meteorite group includes igneous rocks (basalts and cumulates) which generally contain evidence for shock impact metamorphism, such as glass veins and cracks. In the late 70's they were identified to be of possible martian origin (McSween et al., 1979; Wasson and Wetherill, 1979; Wood and Ashwal, 1981), because of their very young radiometric ages of formation. While an impact mechanism to eject the rocks from the martian surface was considered unlikely, the finding of elongated craters at the martian surface strongly suggested that oblique impacts could have removed surface rocks from Mars (Nyquist, 1983). More recently, the SNC ejection mechanism has been explained also for the most common near normal impacts, for crater of hundreds to few km in size (Vickery and Melosh, 1987; Head et al., 2002). Ar, Kr, Xe gases were detected in the glass phase of the shergottite EETA 79001 with relative abundances and isotopic ratios identical to the martian atmosphere (Bogard and Johnson, 1983), providing strong evidence that SNC meteorites were Mars surface crustal mafic materials. Similar measurements performed on other SNC's confirmed the martian origin of this meteorite group (e.g., Marti et al., 1995; Turner et al., 1997). The study in the laboratory of the SNC's, with a combination of infrared spectroscopic, petrologic and geochemical analyses, can add substantial information which is crucial to better understand the origin and evolution of martian surface materials. In particular, the large majority of the spectral investigations are performed to validate and support the remote sensing observations. Pioneering are the early laboratory measurements by Gaffey (1976), who found signatures due to olivines (1.05 μm) and calcium-rich pyroxenes (1.0 and 2.25 μm) for the Chassigny and Nakhla meteorites. This result agrees well with the strong evidence for basalt materials on Mars inferred by the detection of the 1 and 2 μm pyroxene absorption bands in several ground or space-based observational campaigns (e.g., Adams and McCord, 1969; McCord and Westphal, 1971; Bell et al., 1990; Singer and McSween, 1993; Mustard and Sunshine, 1995; Mustard et al., 1997). Other measurements in laboratory were performed in the thermal infrared, the earliest by Sandford (1984), who obtained a good match between Shergotty, Nakhla and Lafayette and terrestrial pyroxene IR transmittance spectra. Salisbury et al. (1991a) performed reflectance and emission spectroscopy on fine powders of ALH77005 and EETA 79001, finding a spectral behavior around 10 μm similar to that of olivine and pyroxene, respectively, that are the main mineral phases of these meteorites. More recently, Hamilton et al. (1997) studied the emissivity of several bulk SNC samples to perform a quantitative study of their mineralogical modes, by applying the linear deconvolution method of Ramsey (1996) to the observed bands. While the near infrared remote observations are consistent with the martian meteorite basalt mineralogy (Mustard and Sunshine, 1995; Mustard et al., 1997), the Middle-Infrared (Mid-IR) spectra from the Thermal Emission Spectrometer (TES) onboard the Mars Global Surveyor spacecraft (Christensen et al., 1992), are not in agreement with the SNC composition: recent analysis of the TES data on a global scale showed that SNC-like compositions are not detected on Mars (Hamilton et al., 2003). The results recalled above obtained on bulk or powdered samples in the spectral range from the visible to the infrared, provided a semi-quantitative average mineralogical characterization of SNC meteorites, which supported the comparison with remote sensing data.

3. Experimental approach

3.1. Sample description

Zagami is a basaltic shergottite that with a crystallization age of 180 Ma (e.g., Shih et al., 1982; Jones, 1986; Nyquist et al., 2001) can be placed among the youngest SNC meteorites, considerably younger than the average martian crust. The space exposure ages of Zagami, suggest that it was ejected from the surface by the same impact event that launched Shergotty, Los Angeles and QUE94201 about 2.7–3.1 Ma ago (Eugster et al., 1996; Nyquist et al., 2001). The meteorite is texturally heterogeneous, with several distinct lithologies dominated by the so-called Normal Zagami (NZ) lithology. In the NZ lithology, pyroxene crystals, with average grain size 0.24–0.36 mm, are arranged with maskelynite grains in a preferential orientation which gives the meteorite its characteristic foliation texture. The average mineral modal, for the NZ lithology varies in the following intervals: pyroxene 70–80%, maskelynite 10–25%, minor phases 4–9% (e.g., Stolper and McSween, 1979; McCoy et al., 1999). Generally, augite and pigeonite occur in equal proportions. Minor phases include phosphate, sulfides and oxides. Few small grains of amphibole are present, especially as trace phases in melt inclusions, typically in pyroxenes.

The sample of Zagami analyzed in this work is a chip characterized by numerous fractures (Fig. 1), of triangular shape (measuring about $5.0 \times 4.5 \times 4.1$ mm) and pertaining to the NZ lithology.

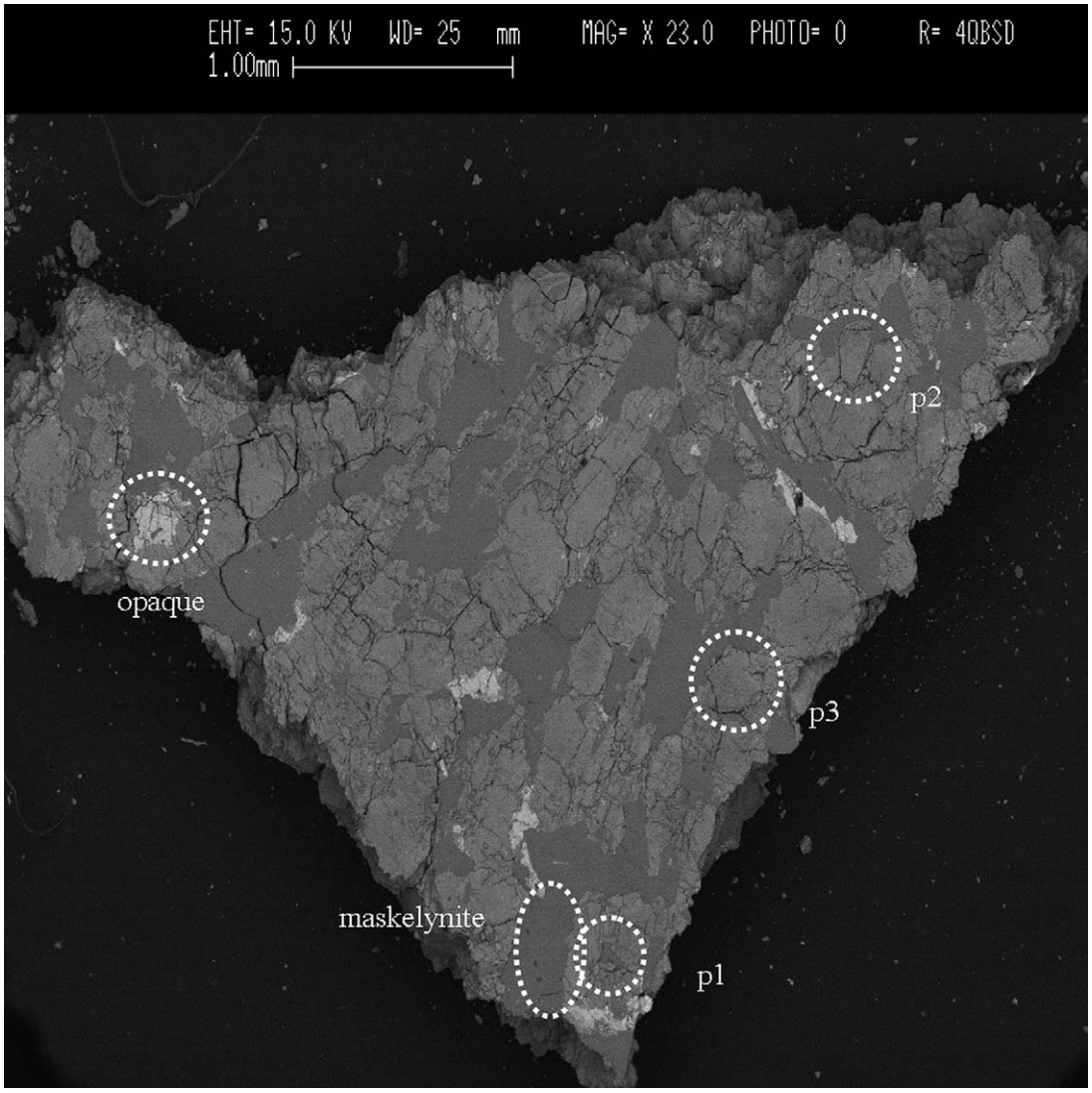

Fig. 1. FESEM image in backscattering mode of the analyzed Zagami chip. White dashed ellipses encircle the regions chosen for the analysis: p1, p2, p3 grains for the pyroxenes, maskelynite and opaque. The different phases in the chip are recognizable by the different gray tones: the opaque phases are the white grains, the pyroxenes are the gray ones and finally the maskelynite are the dark grains. The chip has the dimensions: $5.0 \times 4.5 \times 4.1$ mm.

3.2. Instrumentation

To determine spectral characteristics of our sample in the range 6000–600 cm^{-1} (1.67–16.7 μm) at spectral resolution 4 cm^{-1} we used an infrared microscope attached to a FTIR interferometer (Bruker, Mod. Equinox 55) equipped with a Glowbar lamp as an IR source. The interferometer produces a modulated IR light beam which is directed toward the microscope. Here, after the interaction with the sample (in reflectance or transmittance), the light is collected by the MCT (Mercury–Cadmium–Tellurium) IR detector (cooled by liquid nitrogen). The microscope allows the visual inspection of the sample, for the selection of the area to be analyzed spectroscopically through various interchangeable apertures (from 20 to 400 μm). In the present work, we used the reflectance mode that is bidirectional at phase angle of 0 deg (with incidence angle = emittance angle = 0 deg). For comparison purposes, biconical reflectance measurements at spectral resolution 4 cm^{-1} in the range 6000–400 cm^{-1} were acquired on a large portion of the Zagami fragment by a Graseby Specac accessory placed in the sample chamber of the interferometer. This device allows the measurement of diffuse biconical reflectance by deflecting the radiation towards the sample and by collecting it using two parabolic mirrors. The final reflectance spectrum were retrieved by normalizing the sample spectrum to that of the reference: a KBr powder.

A FESEM (Stereoscan 360 Leica-Cambridge), with nominal spatial resolution 2 nm, was used for sample morphological characterization. The chemical composition was obtained using an EDX analyzer attached to the FESEM for quantitative elemental analysis down to Be. The electron microscope is also equipped with a backscattered electron detector, with resolution 0.1 Z (at Z = 30). IR micro-spectroscopy analyses are non-destructive, while for FESEM analyses, a few nanometer thick chromium coating was applied to avoid sample charging.

Table 1
Elemental analysis, expressed as oxides, for the different grains in Zagami chosen for this study

	This work				McSween and Treiman (1998)		Stolper and McSween (1979)		McCoy et al. (1999)
	p1, low-Ca pyroxene	p2–p3, high-Ca pyroxene	Maske-lynite	Titano-magnetite	Low-Ca pyroxene	High-Ca pyroxene	Maskelynite	High-Ca pyroxene	Titanomagnetite
MgO	19.9	11.9–11.7	–	–	11.09[a]–19.17[b]	11.00[a]–16.00[b]	0.10	11.7[a]–17.0[b]	0.44
Na_2O	–	–	4.7	–	0.08[a]–0.09[b]	0.16[a]–0.18[b]	5.11	–	–
Al_2O_3	1.0	1.3–1.6	29.1	2.4	0.53[a]–0.69[b]	0.93[a]–0.97[b]	27.9	0.90[a]–0.83[b]	2.76
SiO_2	50.4	48.0–46.2	52.2	1.39	49.3[a] – 51.9[b]	50.33[a]–52.08[b]	55.6	50.2[a]–52.0[b]	–
CaO	5.8	14.6–15.9	11.2		6.50[a]–6.35[b]	15.46[a]–16.59[b]	10.7	15.5[a]–16.7[b]	–
FeO	21.7	17.8–17.0	–	65.5	31.67[a]–18.90[b]	21.18[a]–12.09[b]	0.46	19.9[a]–12.2[b]	70.8
TiO_2	–	–	–	22.7	–	–	–	–	22.1

Oxides with sum <1% are not shown. The results by McSween and Treiman (1998), Stolper and McSween (1979) and McCoy et al. (1999) are reported for comparison.
[a] Grain rim.
[b] Grain core.

4. Results

4.1. EDX and backscattered imaging analyses

To report the chemistry of each spot analyzed by micro-spectroscopy we performed EDX and backscattered imaging analyses. Among a large network of fractures, the backscattered image of the Zagami chip (Fig. 1) clearly shows, the presence of two main mineralogies, corresponding to the pyroxene and the maskelynite phase and one minor opaque phase. For these phases we chose sample regions to be investigated by micro-spectroscopy analyses: three sample regions were chosen for the pyroxenes and one region each, for the maskelynite and the opaque. The average chemical composition for all of the five regions (marked in Fig. 1), was obtained in a $\sim(100 \times 100)$ μm^2 window. The chemical data are reported in Table 1 together with results obtained by Stolper and McSween (1979), McSween and Treiman (1998) and McCoy et al. (1999). The three chosen pyroxene grains (p1, p2, p3) show a composition in general good agreement with previous measurements. In fact, p1 appears to be a low-Ca pyroxene (pigeonite), while the p2 and p3 fall in the category of high-Ca pyroxene (augite). The maskelynite appears to have a plagioclase composition with An_{60} and seems to be slightly more Ca-rich than observed by Stolper and McSween (1979) and by McCoy et al. (1999). Finally, the opaque phase shows high concentration of Fe and Ti, with a composition similar to titanomagnetite, with traces of Si, in good agreement with the results obtained by McCoy et al. (1999).

4.2. Spectroscopic investigation

Aperture sizes of less than 250 μm, at a magnification of 300×, were selected to include single mineral grain in the field of view of the microscope. To optimize the S/N ratio, the number of scans for each spectrum was varied between 200 and 500, depending on the reflecting properties of the analyzed area. For each observed region the reflectance measurement, $R(s)$, was repeated four times alternatively to the reflectance of an aluminum mirror, $R(m)$, as reference. The final reflectance spectrum is the average of each $R(s)$ spectrum normalized to $R(m)$. In Fig. 2 we show the pyroxene (p1), the maskelynite, the opaque and the bulk Zagami spectra. The spectral region centered at 1000 cm^{-1}, which for most common planetary materials is dominated by the strong Si–O stretching band, clearly illustrates the diversity of the three mineral phases. Generally, the spectra exhibit different overall band shape and a different location for the Christiansen feature (Cf), that is often used as a compositional parameter (see, e.g., Salisbury and Walter, 1989; Kahle et al., 1993; Salisbury et al., 1997). Salisbury (1993) determined from diffuse reflectance spectra the Cf position for many powdered minerals, finding that the plagioclase Cf varies from about 1234–1285 cm^{-1} (8.1–7.8 μm) for anorthite and albite, respectively and falls at 1176 cm^{-1} (8.5 μm) for augite. The Cf measured in the Zagami spectra falls at 1247 cm^{-1} (8.02 μm) and 1180 cm^{-1} (8.47 μm) for the maskelynite and the pyroxene phase, respectively, in good agreement with Salisbury (1993). Differently from the other phases, the opaque appears almost featureless at 1000 cm^{-1} due to the lack of the SiO molecule in its structure. Comparing the pyroxene and the diffuse reflectance bulk Zagami spectra is evident how the pyroxene phase seems to drive the spectral behavior, while the contribution of maskelynite is not evident. A similar result was obtained by Hamilton et al. (1997) by deconvolving the Zagami bulk spectrum.

5. Discussion

The results presented above show the potential of the IR micro-spectroscopy technique in discriminating single mineral phases in a heterogeneous sample. In the following section we discuss in detail the spectral behavior for each of the different phases identified in our Zagami sample, trying to constrain their chemistry and/or structure. For comparison purposes, spectra of terrestrial mineral samples were acquired by means of the equipment described above or, when not available, were taken from the literature or database sources as cited in the text. We also discuss other spectral features in relation to the presence of volatiles in Zagami.

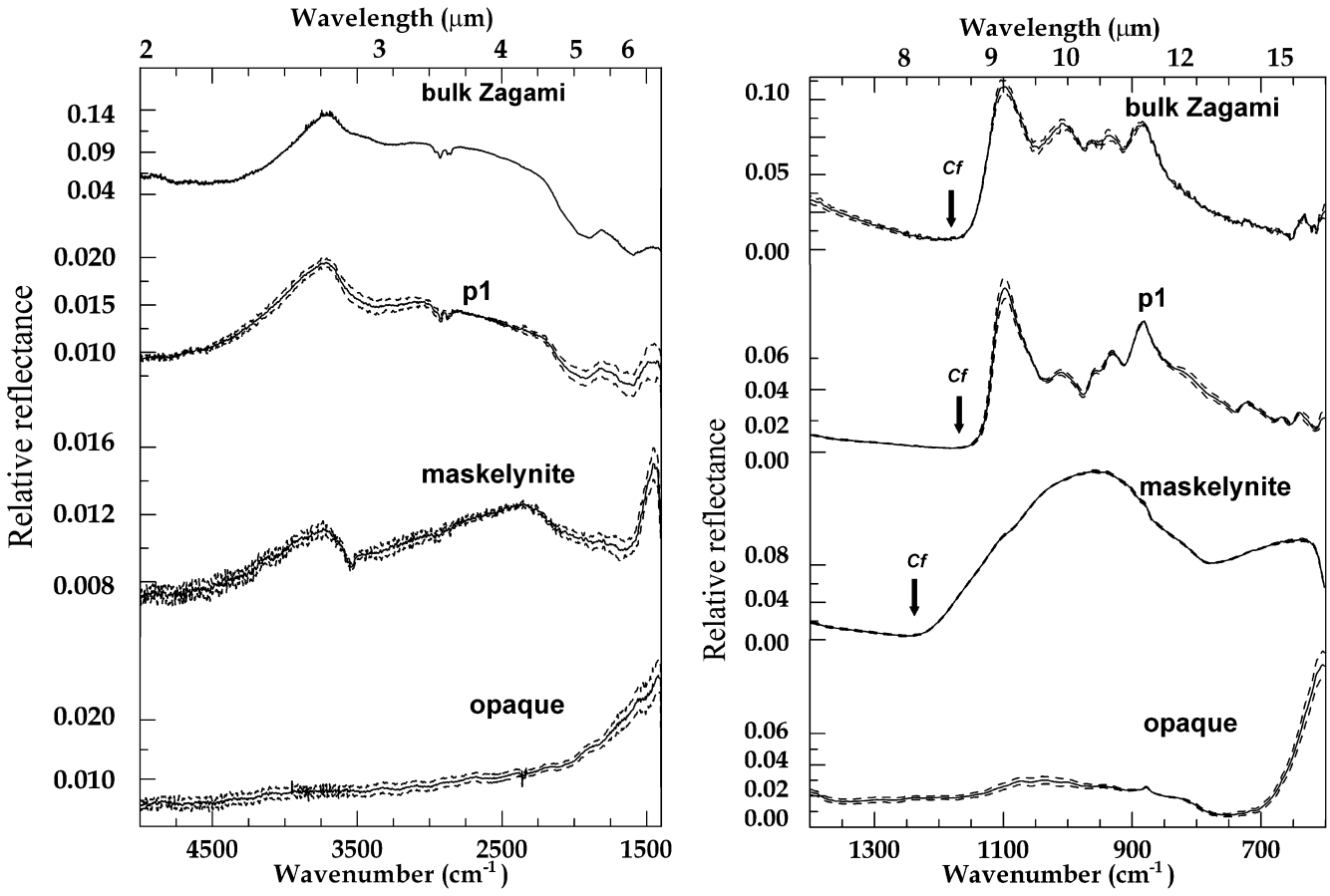

Fig. 2. Micro-IR spectra of the bulk Zagami and the p1, the maskelynite and the opaque grains in the spectral ranges 5000–1400 cm^{-1} (2–7.1 μm) (left) and 1400–600 cm^{-1} (7.1–16.7 μm) (right). The uncertainties of the measurements are shown for each curve as ± the standard deviation (dotted lines). The arrows indicate the position of the Christiansen feature.

5.1. Pyroxenes 1: Mid-IR vs Near-IR

As remembered in Section 2, analysis of the martian surface made in the Middle- or in the Near-IR spectral regions gave some controversial results. When analyzing basaltic material, feldspars and pyroxenes are the main mineral components. The Near-IR allows a fine study of the pyroxene components, while, since strong features are absent in this spectral region, it fails in detecting feldspars. The Mid-IR, by using the deconvolution technique, allows the detection of all the minerals with abundance larger than 10–15 % (Ramsey, 1996). Instead of guessing precisely the mineral member, it gives rather a mineral family composition. The discrepancy between OMEGA and the TES data analysis are an example of the different views that the two spectral interval produce: the OMEGA for the first time revealed vast areas rich in low-Ca pyroxenes, previously undetected by the TES (Bibring et al., 2005; Mustard et al., 2005), but its discovery about soils having a composition similar to SNC was based on the ratio between high- and low-Ca pyroxenes, only. The TES demonstrated, more correctly, that being the Feldspar (and not the pyroxene) the dominant component of martian surface, the connection with SNC fails.

The diversity of the results obtainable by means of the two different spectral regions are evident by examining the pyroxene phases and the bulk Zagami in the whole IR spectral range (see Fig. 3). In the Mid-IR the differences between the high- and low-Ca pyroxene spectra are very weak, making very difficult the discrimination between the different type of pyroxenes. The larger differences are between the single pyroxene grains and the bulk Zagami spectra, probably because of the contribution of the maskelynite to the latter spectrum. In the Near-IR (as discussed in detail in the next paragraph) the discrimination is easier, in fact the three pyroxene grains show distinctive absorption minima in the 2 μm band. In particular, very clear is the different displacement of the band in the low-Ca (p1) and in the high-Ca (p2, p3) pyroxenes. The location of the band in the bulk Zagami spectra represent instead an average value of the several pyroxene phases contributing to the spectrum.

5.2. Pyroxenes 2: low-Ca vs high-Ca

The spectra of the p1, p2, p3 grains, shown in Fig. 4 are characterized by the multi-peak reststrahlen feature, centered around 900 cm^{-1} and extending from about 1150 to 600 cm^{-1}, two absorption bands at 1600 and 1900 cm^{-1}, a broad absorption feature at 3300 cm^{-1}, due to adsorbed water and the hydrocarbon absorption features around 2800–3000 cm^{-1}, due to organic compounds. In Fig. 4, spectra of high-Ca (augite) and Ca-poor (enstatite) pyroxene are shown for comparison. The

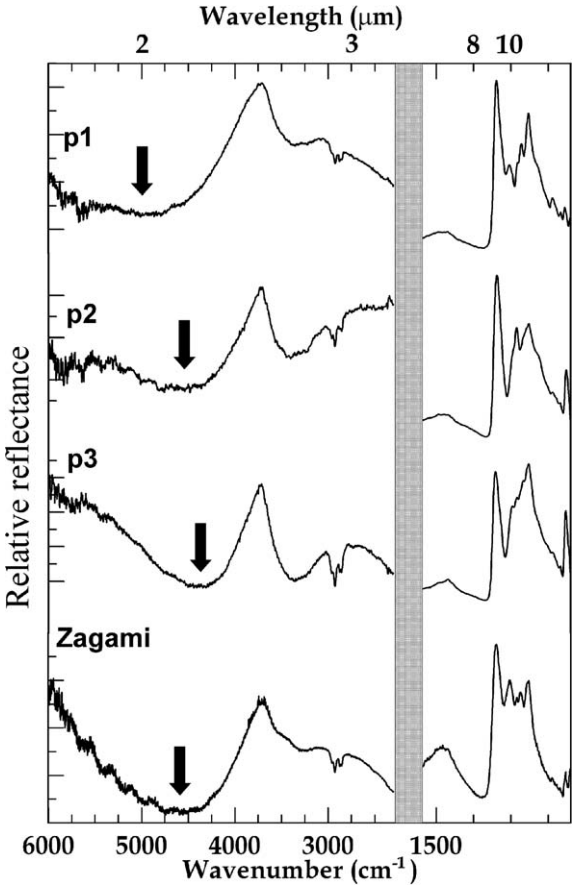

Fig. 3. Micro-IR spectra of p1, p2, p3, and of the bulk Zagami in the spectral range (1.67–16.7 μm). The shaded area divides the Near-IR from the Middle-IR range. The Near-IR spectra are stretched in the Y-axis for clarity. The arrows indicate the position of the 2 μm band minimum.

p2 and p3 spectra are almost identical and resemble well the augite spectrum. The p1 reststrahlen structure shows few weak features: two peaked structures at 930 and 1010 cm^{-1} and two minima at 910 and 975 cm^{-1} not present or slightly discernible in the p2 and p3 spectra. Interestingly, some of these spectral structures are present in the enstatite spectrum and not in the augite one. Similarly, we observe a slight change in the Christiansen feature from 1187 cm^{-1} (8.42 μm) to 1168–1172 cm^{-1} (8.56–8.53 μm) for the p1 and p2, p3, respectively. The corresponding value for the enstatite and augite are 1192 cm^{-1} (8.39 μm) and 1171 cm^{-1} (8.53 μm), quite similar to the values obtained by Salisbury (1993). The spectroscopic results in the Mid-IR (1200–600 cm^{-1}÷8.33–16.7 μm) are confirmed by the EDX measurements, which indicate the p1 grain as a low-Ca pyroxenes and the p2 and p3 as a high-Ca pyroxenes. Additional and stronger spectral evidences that the examined pyroxene grains can be divided in two compositional families of different Ca content comes from the near infrared spectral region. In fact, the 2 μm (5000 cm^{-1}) pyroxenes band can be used to infer on the Ca content (e.g., Adams, 1974; Cloutis and Gaffey, 1991; Sunshine et al., 1990). This band is due to crystal field transitions in the ferrous iron located in the M2 crystallographic site of the pyroxenes (e.g., Burns, 1993 and references therein). Generally, low-Ca orthopyroxenes exhibit a clear spectroscopic trend with the increase of the band minima wavelengths with increasing iron content in the mineral (Cloutis and Gaffey, 1991). Conversely, clinopyroxene spectra are much more variable but for samples containing up to 50 mol% Wo a certain behavior has been determined: the band minima shifts towards longer wavelengths with increasing of Ca content and decreasing of Fe content. Thus, for this category of clinopyroxenes, it is possible, to infer their composition in the En–Fs–Wo system from the wavelengths of the band minima (Cloutis and Gaffey, 1991). Since clinopyroxenes in Zagami fulfill this compositional constraint, we investigated the spectroscopic behavior of the 2 μm band. Although close to the lower wavelength limit of the IR microscope sensitivity, the spectra (Fig. 5) clearly show different absorption band minima for the 2 μm feature: 1.96, 2.27, 2.17 μm, for p1, p2 and p3, respectively. Following the method applied by Schade and Wasch (1999) for Zagami and by Sunshine et al. (1993) for EETA 79001, we extracted our Zagami pyroxene composition from the Cloutis and Gaffey (1991) curves for the pyroxene 2 μm band. The retrieved compositions for the p1, p2 and p3 grains are reported in pyroxene quadrilateral in Fig. 6, together with the results obtained by the EDX analysis for the same grains. The agreement between the two data set is remarkable: the EDX data lay entirely in the compositional area defined by micro-spectroscopy. It should be noted, however, that the p2 and p3 spectrally retrieved compositions have a large common region in which the chemical composition overlaps. This clearly evidence the limits of this technique, that while it can easily discriminate between high- and low-Ca pyroxenes, nevertheless it does not allow a fine determination of the chemical composition, within at least the high-Ca phase. A possible improvement to better constrain the chemical composition could be obtained by using simultaneously the 2 μm and the 1 μm bands.

For a further comparison we plotted in the diagram the compositions by Stolper and McSween (1979) and McSween and Treiman (1998) for the high- and low-Ca phases obtained by Table 1. The good agreement of the three chemical data sets, which form two well defined compositional families with two different levels of Ca content is notable. It should be noted here that IR micro-spectroscopy allows the direct measurement of spectra of individual minerals and chemical composition of the exact same crystal without relying on spectral deconvolution and general geochemical investigations.

The spectra obtained so far can be used for the pyroxene compositional analysis. The results we obtained, verified by EDX analysis, show that analyzing bulk samples by IR microspectroscopy it is possible to measure directly the composition of pyroxenes in the En–Fs–Wo system. This is a significant advance over the state of the art and provides a much more solid foundation for understanding the spectra of martian minerals. However, it should be noted that even in situ spectroscopy could still present spectra of combined minerals, thus deconvolution techniques (such as the MGM, e.g., Sunshine et al., 1993; Schade and Wasch, 1999) should be considered in a complementary manner as a key-tool for separating spectral signatures of individual mineral phases.

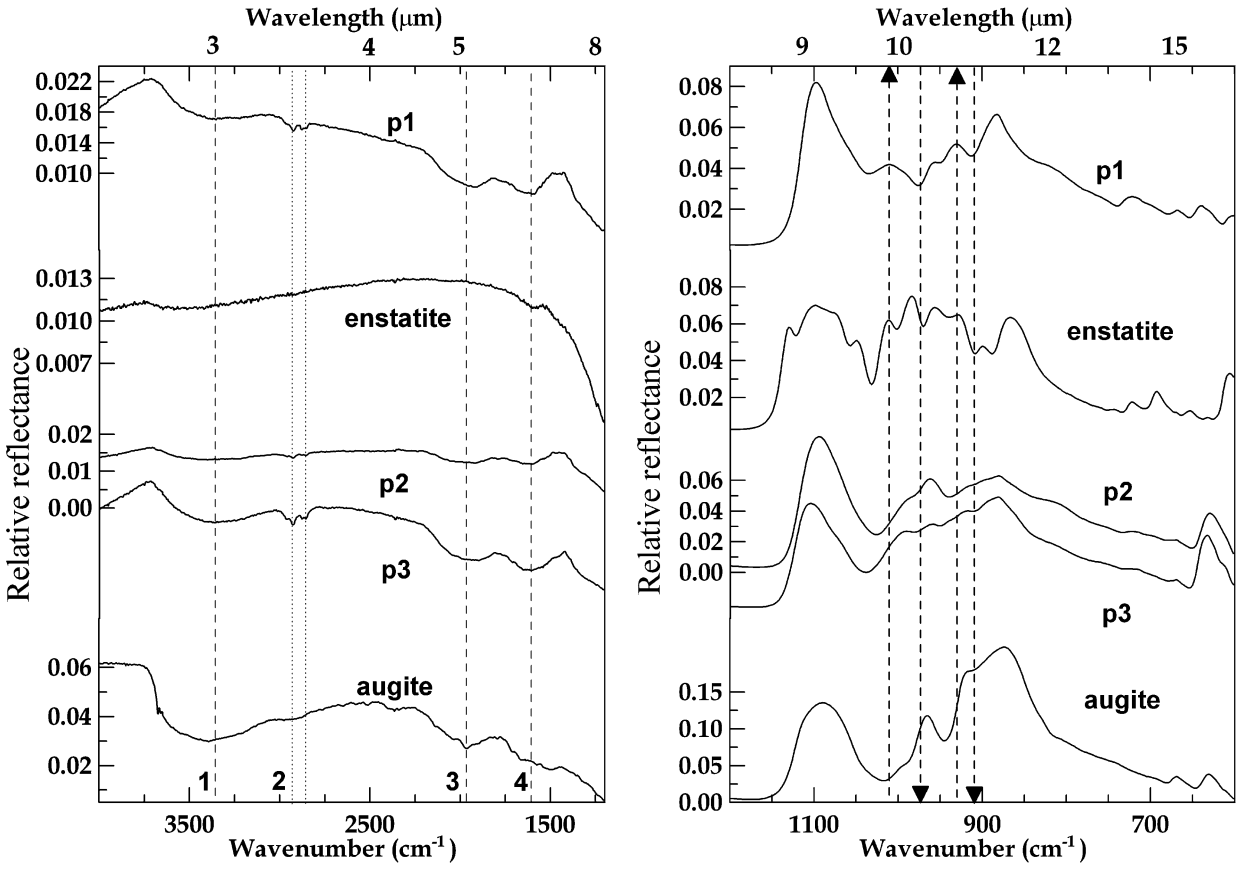

Fig. 4. Micro-IR spectra of p1, p2, p3, terrestrial enstatite and augite grains. (Left) 4000–1200 cm^{-1} (2.5–8.3 μm) spectral range vertical dashed lines indicate the location of hydration (1), hydrocarbon (2), pyroxene 1900 cm^{-1} (5.26 μm) (3) and 1600 cm^{-1} (6.25 μm) (4) absorption features. (Right) 1200–600 cm^{-1} (8.3–16.7 μm) spectral range. Vertical dashed lines, positioned at 910, 930, 975 and 1010 cm^{-1} (respectively 11, 10.7, 10.3 and 9.9 μm), indicate the minor structures common to p1 and enstatite, but lacking in the p2, p3 and augite spectra. In absorption up-arrows and in emissions down-arrows.

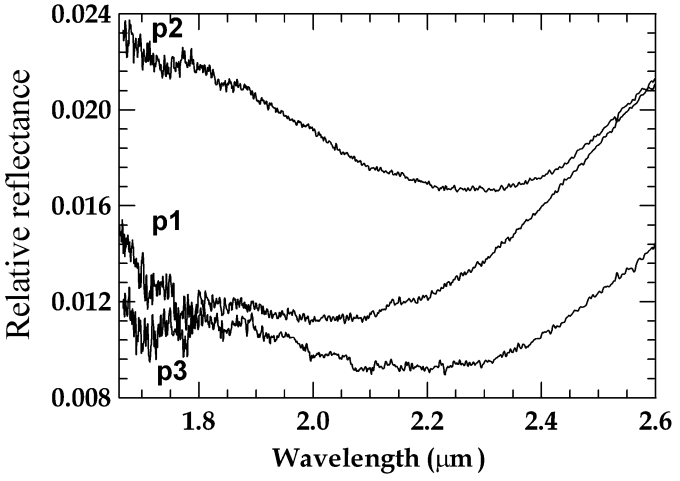

Fig. 5. The pyroxene 2 μm band in the Micro-IR spectra of the p1, p2, p3 Zagami grains.

5.3. Maskelynite

The distinctive feature of the maskelynite is a prominent and broad reststrahlen feature centered at 950 cm^{-1}. Since the maskelynite is an amorphous phase of plagioclase, in Fig. 7 we compare its spectrum with that of terrestrial plagioclases such as labradorite, anorthite and albite. The reststrahlen band of the maskelynite lacks the fine features that conversely are present in the other spectra. This reflects the different atomic arrangement at molecular scale in the maskelynite structure: the amorphization process smears lattice vibrations (Nash and Salisbury, 1991) and, by erasing the high frequency features, produces a smoothing of the band. Thus the maskelynite broad feature testifies to the lack of an ordered crystalline structure.

The position of the Christiansen feature does not change for a crystalline or amorphous plagioclase of the same composition (Nash and Salisbury, 1991), therefore we can compare the Cf position of the maskelynite and the its terrestrial counterparts (Fig. 8). The maskelynite Cf is located at 1247 cm^{-1}, close to that of labradorite (1249 cm^{-1}), while the anorthite Cf is at 1234 cm^{-1} and the albite Cf is located at greater wavenumbers (1285 cm^{-1}). This indicate that the maskelynite is of labradoritic composition as confirmed also by the results obtained from the EDX analysis (An_{60}).

The results obtained so far demonstrate that the IR micro-spectroscopy is able to give information about the atomic arrangement and the composition of the plagioclase phase in the series An–Ab for the maskelynite in Zagami. This means that analyzing bulk samples by IR micro-spectroscopy should be possible to measure directly the composition, by measuring the Cf position, and, directly from the reststrahlen band shape,

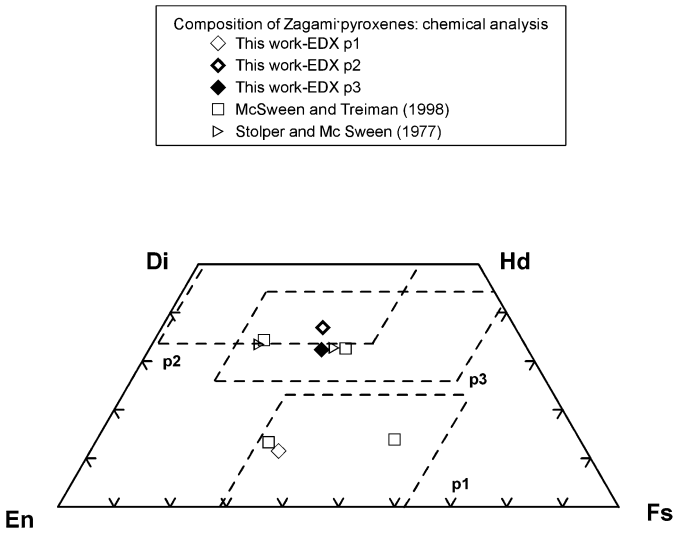

Fig. 6. The composition of the p1, p2, p3, obtained by EDX analyses, plotted (rhombus) on the pyroxene tetralateral diagram (En–Fs–Hd–Di). The data for low-Ca and high-Ca pyroxenes found in Zagami by McSween and Treiman (1998) (squares) and Stolper and McSween (1979) (triangles) are plotted for comparison. Superposed onto the diagram, are the pyroxene compositions (dashed areas) deduced spectroscopically by using the composition vs the 2 μm (5000 cm^{-1}) band position diagram of Cloutis and Gaffey (1991).

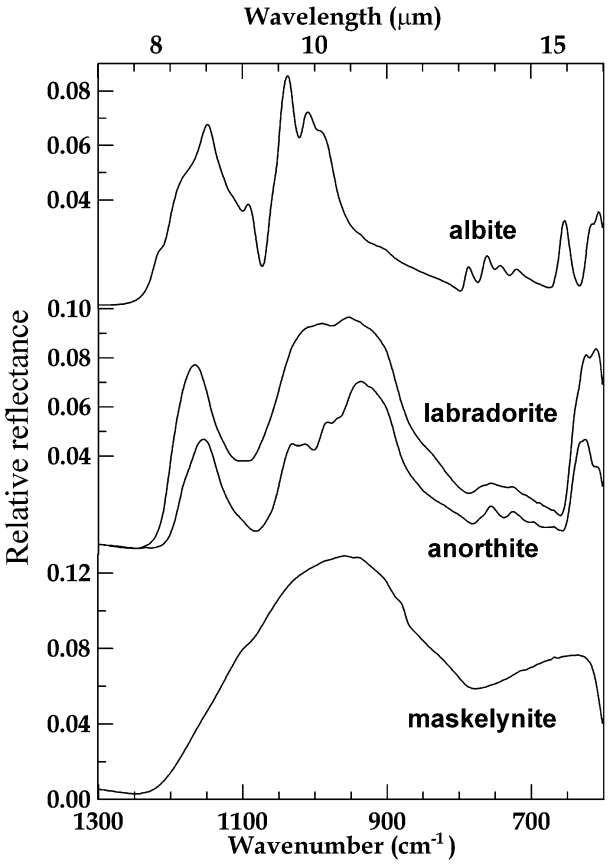

Fig. 7. Spectral comparison in the 1300–600 cm^{-1} (7.7–16.7 μm) range between terrestrial albite, anorthite and labradorite grains with the Zagami maskelynite.

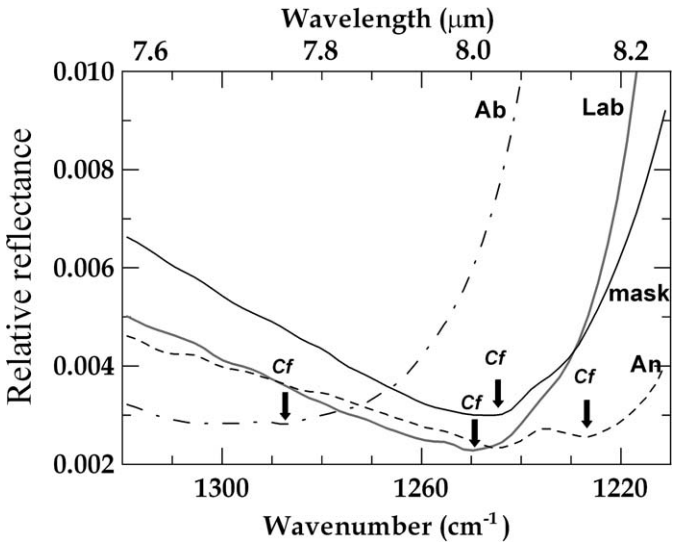

Fig. 8. The Christiansen feature in albite (Ab/dash-dotted line), anorthite (An/dashed line), labradorite (Lab/bolded solid line) and Zagami maskelynite (mask/solid line). The arrows indicate the band positions.

to have indications about the degree of crystallinity (amorphous or crystalline) of a plagioclase phase.

5.4. Titanomagnetite

The spectrum of the opaque appears very flat for $\nu <$ 1500 cm^{-1} ($\lambda >$ 6.67 μm) and almost featureless in the Mid-IR, except for an increasing slope and for a broad and weak feature between 800 and 1100 cm^{-1}, due to possible spectral contamination of the nearby pyroxene. This spectral behavior resembles that of oxide materials, whose main strong peaks are at wavenumbers < 600–700 cm^{-1}. The spectrum of the opaque is compared in Fig. 9 with that of ilmenite and magnetite, two oxides having a strong affinity with titanomagnetite. Similarly to the opaque grain, the spectra of the two oxides are very flat up to about 700–800 cm^{-1}, where the overall reflectance increases. However, it should be noted that the steep slope of the opaque spectrum shortward of 700 cm^{-1} is more similar to the ilmenite spectral behavior rather than the magnetite one.

5.5. Volatiles

The pyroxene and maskelynite spectra in Zagami present well defined features due to volatile materials. In this section we will study their characteristics in order to try to infer hypothesis about their origin. Firstly, we will compare the absorption band areas that should be linked to the abundance of the volatiles adsorbed onto these two different mineral phases. Furthermore, we will compare the CH composite structure present in different terrestrial and extraterrestrial materials with the ones in Zagami.

The detection of water and organics features by (reflectance) spectroscopy of powdered/solid materials is, in general, a tricky task (e.g., Salisbury, 1993). Expected to be present only in carbonaceous chondrites, water and organic stretching bands of variable intensities were found in the majority of the studied

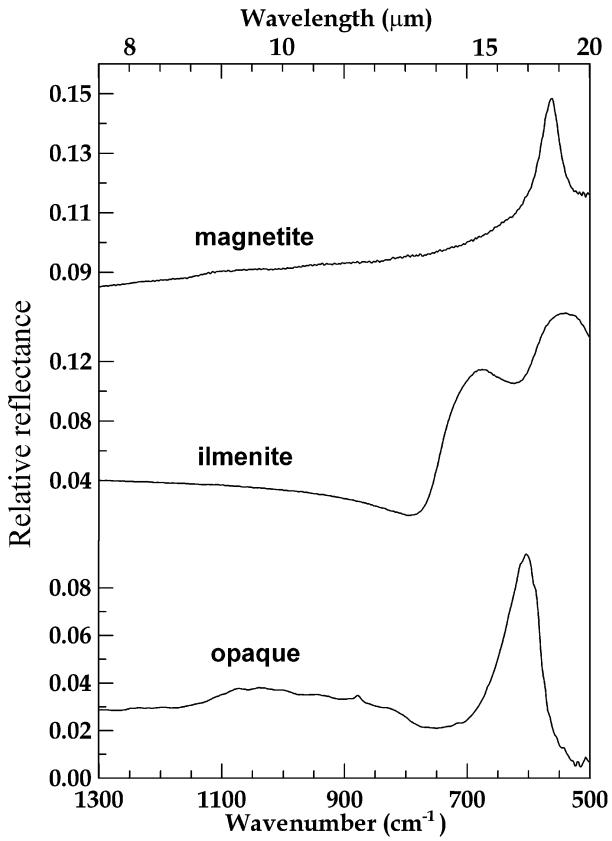

Fig. 9. Spectral comparison in the range 1300–600 cm^{-1} (7.7–16.7 μm) between terrestrial magnetite and ilmenite from Salisbury et al. (1991b), with the Zagami opaque phase.

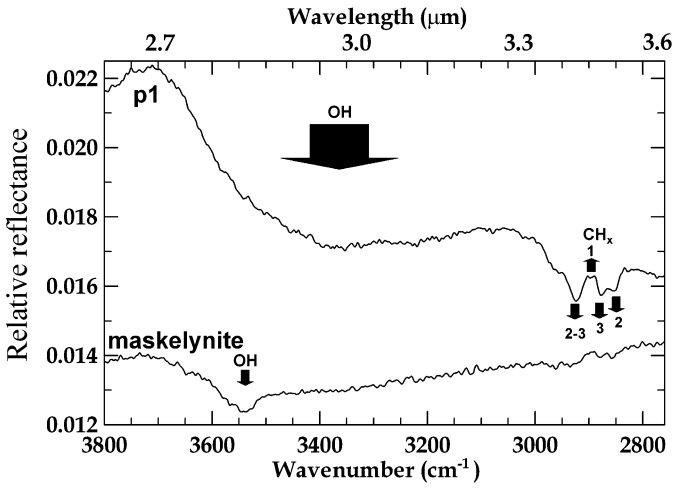

Fig. 10. The p1, p2 and maskelynite spectra in the range of the volatile features (3800–2700 cm^{-1}) (2.6–3.7 μm). Aliphatic hydrocarbon and water signatures are marked.

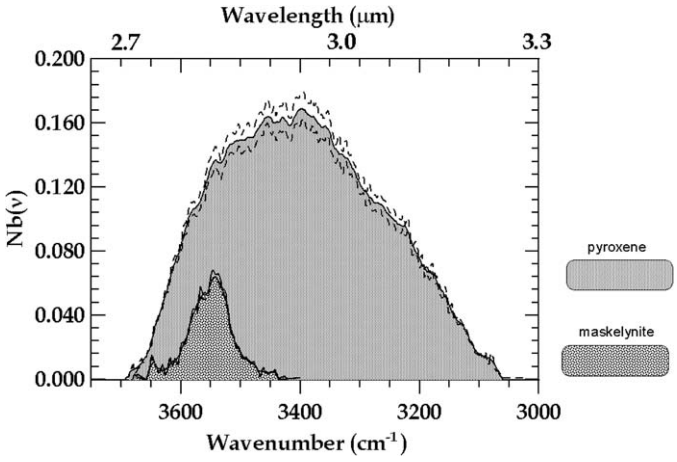

Fig. 11. The normalized band of hydration, $Nb(\nu)$, for pyroxene and maskelynite in Zagami.

SNC meteorites (e.g., Sandford, 1984; Salisbury et al., 1991a; Bishop et al., 1998a). Terrestrial weathering or contamination is the most plausible explanation for these features, although an indigenous origin cannot be ruled out a priori.

Martian meteorites show little evidence of hydration. Nevertheless, most of them show a prominent O–H fundamental vibration band at 3500 cm^{-1}, possibly due to sample contamination. Water hydration bands were observed in the Lafayette, Nakhla and Shergotty (Sandford, 1984), ALH7705 and EETA 79001 (Salisbury et al., 1991a) and ALH84001 (Bishop et al., 1998a, 1998b) SNC meteorites. Our Zagami spectra (Fig. 10) show hydration features associated with pyroxenes (in the interval 3100–3600 cm^{-1}) and maskelynite (at about 3540 cm^{-1}). To estimate the relative amounts of bound water in pyroxene and maskelynite, we calculated the band areas associated with the O–H features. First of all, we normalized the O–H band to the reflectance of the continuum defined as a linear fit at the band edge, as: $Nb(\nu) = (Rc(\nu) - Rb(\nu))/Rc(\nu)$, where $Rb(\nu)$ is the reflectance in the band. At the band center, $\nu = \nu_o$, according to Clark and Roush (1984), is possible to obtain the band depth. Due to the different location of the water band in the two phases, we used two different spectral ranges, i.e., 3050–3650 cm^{-1} for the pyroxene and 3400–3680 cm^{-1} for the maskelynite band. The resulting normalized pyroxene and maskelynite bands are shown in Fig. 11. The ratio of the pyroxene to the maskelynite band areas (the shaded regions in Fig. 11) is about 12, confirming a weaker absorption and suggesting that the glass is drier than the pyroxenes.

With regard to the organic matter, Salisbury et al. (1991a) suggest that indigenous aliphatic compounds are only in carbonaceous chondrites. However, Bishop et al. (1998a) suggested a possible martian origin for organics found in ALH84001, after the comparison between aliphatic hydrocarbon features present in the meteorite and those of several laboratory contaminants.

The pyroxene spectrum clearly shows a multiple absorption in the range 2800–2960 cm^{-1}, where the fundamental C–H stretching vibrations occur for aliphatic hydrocarbon, i.e., hydrocarbon groups in which the carbon atom is singly bonded to the other atoms (CH_3, CH_2, CH) (Allamandola et al., 1992). Fig. 10 evidences that CH, CH_2 and CH_3 stretching bands at 2898, 2855–2926 and 2876–2958 cm^{-1}, respectively, are present in the pyroxene spectrum, while they are nearly absent in the maskelynite spectrum. To quantify the presence of the organic relatively at the two mineral phase we follow the same procedure used above for the O–H absorption band. The nor-

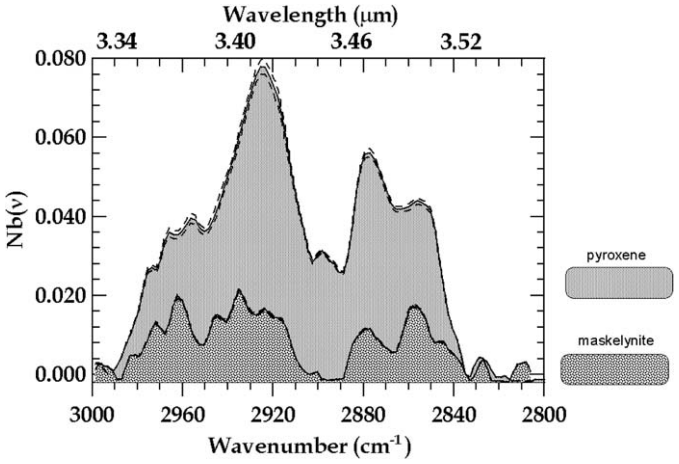

Fig. 12. The normalized aliphatic bands, $Nb(\nu)$, for pyroxene and maskelynite in Zagami.

malized C–H bands, taken in the interval 2830–2990 cm^{-1}, are shown in Fig. 12, for the pyroxene and the maskelynite. In this case the ratio of the pyroxene to the maskelynite band areas (the shaded regions in figure) is about 4.

Our results indicate that pyroxene is richer in water and organics than maskelynite. A variation in the water and organic bands across the chip of the ALH84001 meteorite brought Bishop et al. (1998a) to suggest that these features were due to heterogeneous components in the meteorite and not to laboratory contamination. Our results for Zagami, not only confirm this kind of variations across the sample but also explain that the hydration and organic signatures are confined chiefly to the pyroxene grains. This could be a more stringent indication that the organic and water features in Zagami are due to heterogeneous compounds rather than to a contamination. Another possibility is that the mineral structures of pyroxenes are just more accommodating and thus more susceptible to adsorbed contamination than maskelynite. Indications on the peculiar nature of the aliphatic structure in Zagami can be extracted by the spectra of samples possibly contaminated by the organics and water vapor present in the laboratory environment. In Fig. 13 we present the spectra of pyroxenes, plagioclases, and the Murchison meteorite, an organic rich extraterrestrial material. In addition, we show reflectance spectra from Salisbury et al. (1991b), who also addressed the problem of the laboratory contamination of some of their samples. The spectra from our laboratory were measured both by micro-spectroscopy and by biconical reflectance. As shown in Fig. 13, the laboratory aliphatic contamination has a similar shape in both the measurements configurations (Micro-IR and biconical reflectance) and for different investigators (Salisbury et al., 1991b, and us).

Although the Murchison meteorite contains indigenous organic matter it exhibits an aliphatic structure very similar to the contaminated materials, which makes difficult to decide about the origin of this feature.

Conversely, the Zagami pyroxene aliphatic structure appear to be quite different from the other investigated materials, showing a unique feature at 2876 cm^{-1} (indicated by an arrow), due

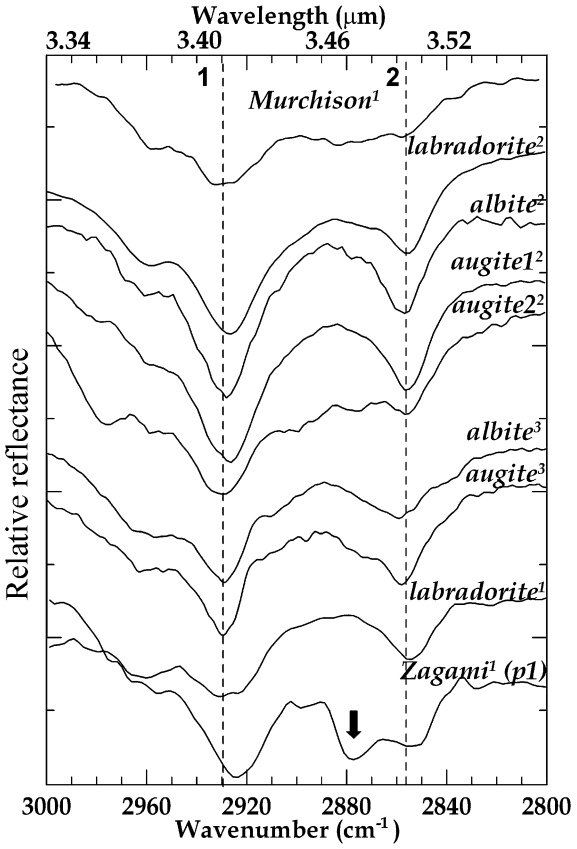

Fig. 13. Aliphatic spectral structure in different materials and for different measurement techniques. Label 1 indicates measurement by Micro-IR. Label 2 is used for diffuse reflectance spectra of materials in the size range (0–75 μm) taken from Salisbury et al. (1991b). Label 3 indicates biconical reflectance spectra of albite (0–20 μm) and augite (100–200 μm), measured by us. The lines labeled 1 and 2 indicate the absorption bands due to the CH_2.

to the CH_3, that is missing in all the other investigated materials. In addition, it exhibits the two strong bands (labeled 1 and 2 in the figure) which are common also to Murchison and the other materials, but these features are slightly shifted towards lower wavenumbers.

The discussion above seems to indicate that the aliphatic structure observed in Zagami, or at least the 2876 cm^{-1} CH_3 feature, is not likely due to a common laboratory contaminant. Nevertheless, further investigations are mandatory to the conclusive assignment of the organic signature origins in Zagami.

6. Conclusions

We have analyzed a mm-size chip of Zagami. For the first time, thanks to the IR micro-spectroscopy analytical technique (6000–600 $cm^{-1} \div 1.67$–16.7 μm) it has been possible to extract individually the infrared spectra of the major mineral phases in Zagami, i.e., the pyroxenes and the maskelynite. A minor oxide phase, found in many SNC's, was also observed. In the reststrahlen region, the discrimination between the high-Ca and low-Ca pyroxene spectra is possible even if difficult, due to very minor differences in the main vibration band. However, both the Zagami pyroxene spectral signatures match well the spec-

tra of chemically-similar terrestrial pyroxenes. The study of the 2 μm band minima makes it possible to clearly discriminate between the two Zagami pyroxene families, i.e., high- and low-Ca pyroxenes. The chemical composition as inferred by spectroscopic techniques is in good agreement with the composition measured directly by the EDX detection system. The IR microspectroscopy allowed the direct detection between the high- and low-Ca phases, in a igneous bulk sample. Thanks to the results presented here we can state that infrared micro-spectroscopy is a promising, non-destructive, technique to study pyroxene compositions in bulk samples.

A spectral comparison with terrestrial samples and with EDX chemical data confirms composition and the lack of crystalline structure for the plagioclase phase in Zagami. The study of the Christiansen feature position, which falls at wavenumbers typical of labradorite is in very good agreement with the EDX-retrieved composition for the plagioclase glass (An_{60}). Spectral signatures due to water and organics have been detected separately in the pyroxenes and the maskelynite. A clear enrichment of volatiles in the pyroxene were measured. The fact that the hydration and organic signatures were found predominantly in the pyroxene, and that similar organic features are not seen in terrestrial pyroxenes measured under the same conditions, could exclude the terrestrial contamination as the origin for these features. This result opens new scenarios for understanding the origin of these features, however more definitive studies are needed, e.g., the study of other SNC meteorites in a similar fashion.

This work demonstrates the potential application of the IR micro-spectroscopy technique, which should be considered in the perspective of future "in situ" space research (e.g., Capaccioni et al., 2001; Lamartinie et al., 2003). In fact, for the first time, this technique has been used to unambiguously identify different mineralogical phases in a heterogeneous sample. In addition, it has been combined with a direct chemical detection technique (EDX) thus validating its reliability as mineralogical investigation tool. Considering the complexity of the results interpretation, laboratory work performed by means of the IR micro-spectroscopy technique represents a reference tool for the interpretation of future in situ analyses.

Acknowledgments

We want to thank warmly Prof. Frans J.M. Rietmeijer for very constructive discussions during the preparation of the manuscript. We thank E. Zona, N. Staiano and S. Inarta for their technical assistance during experiment execution. We thank M. Minniti, T. McCoy for their critical and friendly suggestions. Comments and suggestions of the referees, Ted Roush and Jessica Sunshine, are gratefully acknowledged. This work was supported by MIUR, ASI.

References

Allamandola, L.J., Sandford, S.A., Tielens, A.G.G.M., Herbst, T.M., 1992. Infrared spectroscopy of dense clouds in the C–H stretch region—Methanol and 'diamonds.' Astrophys. J. 399, 134–146.

Adams, J.B., 1974. Visible and near-infrared diffuse reflectance spectra of pyroxenes as applied to remote sensing of solid objects in the Solar System. J. Geophys. Res. 79, 4829–4836.

Adams, J.B., McCord, T.B., 1969. Mars: Interpretation of spectral reflectivity of light and dark regions. J. Geophys. Res. 74, 4851–4856.

Bell III, J.F., McCord, T.B., Owensby, P.D., 1990. Observational evidence of crystalline iron oxides on Mars. J. Geophys. Res. 95, 14447–14461.

Bibring, J.-P., Langevin, Y., Gendrin, A., Gondet, B., Poulet, F., Berthé, M., Soufflot, A., Arvidson, R., Mangold, N., Mustard, J., Drossart, P., 2005. Mars surface diversity as revealed by the OMEGA/Mars Express Observations. Science 307, 1576–1581.

Bishop, J.L., Pieters, C.M., Hiroi, T., Mustard, J.F., 1998a. Spectroscopic analysis of martian meteorite Allan Hills 84001 powder and applications for spectral identification of minerals and other soil components on Mars. Meteorit. Planet. Sci. 33, 668–707.

Bishop, J.L., Mustard, J.F., Pieters, C.M., Hiroi, T., 1998b. Recognition of minor constituents in reflectance spectra of Allan Hills 84001 chips and the importance for remote sensing on Mars. Meteorit. Planet. Sci. 33, 693–698.

Bogard, D.D., Johnson, P., 1983. Martian gases in an Antarctic meteorite? Science 221, 651–654.

Burns, R.G., 1993. Electronic spectra. In: Pieters, C.M., Englert, P.A.J. (Eds.), Remote Geochemical Analysis: Elemental and Mineralogical Composition. Cambridge Univ. Press, New York, pp. 3–29.

Capaccioni, F.G., and 21 colleagues, 2001. MARS-IRMA: In-situ infrared microscope analysis of martian soil and rock samples. Adv. Space Res. 28, 1219–1224.

Christensen, P.R., and 10 colleagues, 1992. Thermal emission spectrometer experiment: Mars Observer Mission. J. Geophys. Res. 97, 7719–7734.

Clark, R.N., Roush, T.L., 1984. Reflectance spectroscopy: Quantitative analysis techniques for remote sensing applications. J. Geophys. Res. 89, 6329–6340.

Cloutis, E.A., Gaffey, M.J., 1991. Spectral-compositional variations in the constituent minerals of mafic and ultramafic assemblages and remote sensing implications. Earth Moon Planets 53, 11–53.

Eugster, O., Weigel, A., Polnau, E., 1996. Two different ejection events for basaltic shergottites QUE94201, Zagami and Shergotty (2.6 Ma Ago) and lherzolitic shergottites LEW88516 and ALH77005 (3.5 Ma Ago). Lunar Planet. Sci. 27, 345–346.

Gaffey, M.J., 1976. Spectral reflectance characteristics of the meteorite classes. J. Geophys. Res. 81, 905–920.

Hamilton, V.E., Christensen, P.R., McSween Jr., H.Y., 1997. Determination of martian meteorite lithologies and mineralogies using vibrational spectroscopy. J. Geophys. Res. 102, 25581–25592.

Hamilton, V.E., Christensen, P.R., McSween Jr., H.Y., Bandfield, J.L., 2003. Searching for the source regions of martian meteorites using MGS TES: Integrating martian meteorites into the global distribution of igneous materials on Mars. Meteorit. Planet. Sci. 38, 871–885.

Head, J.N., Melosh, H.J., Ivanov, B.A., 2002. Martian meteorite launch: High speed ejecta from small craters. Science 298, 1752–1756.

Jones, J.H., 1986. A discussion of isotopic systematics and mineral zoning in the shergottites: Evidence for a 180 m.y. igneous crystallization age. Geochim. Cosmochim. Acta 50, 969–977.

Kahle, A.B., Palluconi, F.D., Christensen, P.R., 1993. Thermal emission spectroscopy: Application to the Earth and Mars. In: Pieters, C.M., Englert, P.A.J. (Eds.), Remote Geochemical Analysis: Elemental and Mineralogical Composition. Cambridge Univ. Press, New York, pp. 99–120.

Klima, R.L., Pieters, C.M., 2005. Capabilities and limitations of infrared reflectance micro-spectroscopy. Lunar Planet. Sci. 35. Abstract 1307 [CD-ROM].

Lamartinie, S., Bibring, J.-P., Soufflot, A., 2003. Definition of the active cooling system for the space instrument CIVA/Mars. In: Proc. SPIE, vol. 4850, pp. 1109–1119.

Marti, K., Kim, J.S., Thakur, A.N., McCoy, T.J., Keil, K., 1995. Signatures of the martian atmosphere in glass of Zagami meteorite. Science 267, 1981–1984.

McCord, T.B., Westphal, J.A., 1971. Mars: Narrow-band photometry, from 0.3 to 2.5 microns, of surface regions during the 1969 apparition. Astrophys. J. 168, 141–154.

McCoy, T.J., Wadhwa, M., Keil, K., 1999. New lithologies in the Zagami meteorite: Evidence for fractional crystallization of a single magma unit on Mars. Geochim. Cosmochim. Acta 63, 1249–1262.

McSween Jr., H.Y., Treiman, A.H., 1998. Martian meteorites. In: Papike, J.J. (Ed.), Planetary Materials. In: Reviews in Mineralogy, vol. 36. Min. Soc. of America. Chap. 6.

McSween Jr., H.Y., Stolper, E.M., Taylor, L.A., Muntean, R.A., O'Kelley, G.D., Eldridge, J.S., Biswas, S., Ngo, H.T., Lipschutz, M.E., 1979. Petrogenetic relationship between Allan Hills 77005 and other achondrites. Earth Planet. Sci. Lett. 45, 275–284.

Morlok, A., Jones, G.C., Grady, M.M., 2004. FT-IR micro-spectroscopy of fine-grained planetary materials: Further results. Lunar Planet. Sci. 35. Abstract 1622 [CD-ROM].

Mustard, J.F., Sunshine, J.M., 1995. Seeing through the dust on Mars: Links between the SNC meteorites and heterogeneity on the surface of the Red Planet. Science 267, 1623–1626.

Mustard, J.F., Murchie, S.L., Erard, S., Sunshine, J.M., 1997. In situ compositions of martian volcanics: Implications for the mantle. J. Geophys. Res. 102, 25605–25615.

Mustard, J.F., Poulet, F., Gendrin, A., Bibring, J.-P., Langevin, Y., Gondet, B., Mangold, N., Bellucci, G., Altieri, F., 2005. Olivine and pyroxene diversity in the crust of Mars. Science 307, 1594–1597.

Nash, D.B., Salisbury, J.W., 1991. Infrared reflectance spectra of plagioclase feldspars. Geophys. Res. Lett. 18, 2145–2147.

Nyquist, L.E., 1983. Do oblique impacts produce martian meteorites? Proc. Lunar Sci. Conf. 13. J. Geophys. Res. 88 (1983) 785–798.

Nyquist, L.E., Bogard, D.D., Shih, C.-Y., Greshake, A., Stoffler, D., Eugster, O., 2001. Ages and geologic histories of martian meteorites. Space Sci. Rev. 96, 105–164.

Ramsey, M.S., 1996. Object detection utilizing a linear retrieval algorithm for thermal infrared imagery. In: Proc. 2nd. Int. Airborne Rem. Sens. Conf., San Francisco, CA, vol. 2, pp. 559–569.

Salisbury, J.W., 1993. Mid-infrared spectroscopy: Laboratory data. In: Pieters, C.M., Englert, P.A.J. (Eds.), Remote Geochemical Analysis: Elemental and Mineralogical Composition. Cambridge Univ. Press, New York, pp. 79–98.

Salisbury, J.W., Walter, L.S., 1989. Thermal infrared (25–13.5 μm) spectroscopic remote sensing of igneous rock types on particulate planetary surfaces. J. Geophys. Res. 94, 9192–9202.

Salisbury, J.W., D'Aria, D.M., Jarosewich, E., 1991a. Mid-infrared (25–13.5 μm) reflectance spectra of powdered stony meteorites. Icarus 92, 280–297.

Salisbury, J.W., Walter, L.S., Vergo, N., D'Aria, D.M., 1991b. Mid-infrared (21–25 μm) spectra of minerals. Johns Hopkins Univ. Press, Baltimore.

Salisbury, J.W., Basu, A., Fischer, E.M., 1997. Thermal infrared spectra of lunar soils. Icarus 130, 125–139.

Sandford, S.A., 1984. Infrared transmission spectra from 25 to 25 μm of various meteorite classes. Icarus 60, 115–126.

Schade, U., Wasch, R., 1999. Near-infrared reflectance spectra from bulk samples of two martian meteorites Zagami and Nakhla. Meteorit. Planet. Sci. 34, 417–424.

Shih, C.Y., Nyquist, L.E., Bogard, D.D., MCKay, G.A., Wooden, J.L., Bansal, B.M., Wiesmann, H., 1982. Chronology and petrogenesis of young achondrites, Shergotty, Zagami and ALHA77005: Late magmatism on a geologically active planet. Geochim. Cosmochim. Acta 46, 2323–2344.

Singer, R.B., McSween Jr., H.Y., 1993. The igneous crust of Mars: Compositional evidence from remote sensing and the SNC meteorites. In: Lewis, J., Matthews, M.S., Guerrieri, M.L. (Eds.), Resources of Near Earth Space. Univ. of Arizona Press, Tucson, AZ, pp. 709–736.

Stolper, E., McSween Jr., H.Y., 1979. Petrology and origin of the shergottite meteorites. Geochim. Cosmochim. Acta 43, 1475–1498.

Sunshine, J.M., Pieters, C.M., Pratt, S.F., 1990. Deconvolution of mineral absorption bands: An improved approach. J. Geophys. Res. 95, 6955–6966.

Sunshine, J.M., McFadden, L.-A., Pieters, C.M., 1993. Reflectance spectra of the Elephant Moraine A79001 meteorite: Implications for remote sensing of planetary bodies. Icarus 105, 79–91.

Suzuki, A., Kebukawa, Y., Nakashima, S., Keller, L.P., Zolensky, M.E., Nakamura, T., 2005. Infrared micro-spectroscopy of organic and hydrous components in some antarctic micro-meteorites. Lunar Planet. Sci. 36. Abstract 1176 [CD-ROM].

Turner, G., Knott, S.F., Ash, R.D., Gilmour, J.D., 1997. Ar–Ar chronology of the martian meteorite ALH84001: Evidence for the timing of the early bombardment of Mars. Geochim. Cosmochim. Acta 61, 3835–3850.

Vickery, A.M., Melosh, H.J., 1987. The large crater origin of SNC meteorites. Science 237, 738–743.

Wasson, J., Wetherill, G., 1979. Dynamical, chemical, and isotopic evidence regarding the formation locations of asteroids and meteorites. In: Gehrels, T. (Ed.). Asteroids, Univ. of Arizona Press, Tucson, AZ, pp. 926–974.

Wood, C.A., Ashwal, L.D., 1981. SNC meteorites: Igneous rocks from Mars? Proc. Lunar Sci. Conf. 12, 1359–1375.